Nonuniformity correction of infrared cameras by reading radiance temperatures with a spatially nonhomogeneous radiation source

OPEN ACCESS
IOP Publishing
Measurement Science and Technology
Meas. Sci. Technol. **28** (2017) 015401 (14pp)
doi:10.1088/1361-6501/28/1/015401

Nonuniformity correction of infrared cameras by reading radiance temperatures with a spatially nonhomogeneous radiation source

Berndt Gutschwager and Jörg Hollandt

Physikalisch-Technische Bundesanstalt (PTB), Abbestr. 2-12, 10587 Berlin, Germany

E-mail: Berndt.Gutschwager@PTB.de

Received 30 June 2016, revised 25 October 2016
Accepted for publication 4 November 2016
Published 28 November 2016

Abstract

We present a novel method of nonuniformity correction (NUC) of infrared cameras and focal plane arrays (FPA) in a wide optical spectral range by reading radiance temperatures and by applying a radiation source with an unknown and spatially nonhomogeneous radiance temperature distribution. The benefit of this novel method is that it works with the display and the calculation of radiance temperatures, it can be applied to radiation sources of arbitrary spatial radiance temperature distribution, and it only requires sufficient temporal stability of this distribution during the measurement process. In contrast to this method, an initially presented method described the calculation of NUC correction with the reading of monitored radiance values. Both methods are based on the recording of several (at least three) images of a radiation source and a purposeful row- and line-shift of these sequent images in relation to the first primary image. The mathematical procedure is explained in detail. Its numerical verification with a source of a predefined nonhomogeneous radiance temperature distribution and a thermal imager of a predefined nonuniform FPA responsivity is presented.

Keywords: imaging systems, thermal imaging, detectors, cameras, focal-plane-array image processors

(Some figures may appear in colour only in the online journal)

1. Introduction

A novel first method of nonuniformity correction of focal plane array (FPA)-based imaging systems and imaging systems with other detector layouts in a broad optical spectral range by applying a radiation source with an unknown and spatially nonhomogeneous radiance temperature distribution was described in [1]. Imagers and particularly FPA-based imagers in the visible and infrared spectral range are widely used in technical fields such as radiometry, photometry, condition monitoring, process control, remote sensing, defense, surveillance, medical imaging and health care [2]. Especially infrared FPAs suffer significantly from a nonuniformity of the response of the individual detectors of the array [3]. This FPA-non-uniformity is generally described by a linear model that attributes an individual gain and offset to the response of each detector of the array to its received irradiance. Gain and offset vary spatially across the array and they also generally vary in time, due to detector degradation, in terms of the environmental conditions (i.e. surrounding temperature) and the radiance temperature of the observed object. This nonuniformity of the FPA results in image errors superimposed on the true image which are called fixed pattern noise (FPN).

For infrared FPAs the responsivity nonuniformity is their major performance limitation. It degrades the image quality, radiometric accuracy and thermal resolution. Thus the non-uniformity correction (NUC) is an essential part of the metrological characterization and calibration of infrared thermal imagers during the initial factory calibration process and regularly during their operation in the field.

Generally, large-area radiators, e.g. thermal plate radiators in the infrared or integrating spheres in the visible spectral range which completely fill the field-of-view of the imaging system, are applied to the NUC. However, large-area thermal plate radiators show a nonhomogeneous radiance and radiation temperature distribution across their surface [4]. This non-homogeneity directly limits their applicability for the NUC. To avoid this inherent limitation of plate radiators, individual measurements of the existing radiance non-homogeneity across their radiating surface can be performed for all relevant temperatures [5]. This procedure leads to very accurate results and it is shown in [4] that it allows for example, a NUC with 104 mK uncertainty at a radiance temperature of 100 °C for an infrared imager equipped with an MCT, QWIP detector array of 320 × 256 pixels. However, this procedure is only applicable in the laboratory, is very time consuming and requires a high-grade radiation thermometer. In the case of rapid and in-field NUCs, this method cannot be applied.

In the following we present a novel method [6] of how the NUC of an imager can be performed accurately on a source with an unknown and spatially nonhomogeneous radiance temperature distribution if only the source shows a sufficient temporal stability to record a series of several (at least three) images by a purposeful row- and line-shift of these sequent images in relation to the first primary image.

2. Description of method of nonuniformity correction

For the NUC with a source of arbitrary radiance temperature distribution, two different variants can be distinguished when applying an imager which records radiance temperature values.

The NUC is performed on the basis of three successively taken images of the radiation source. A first image is taken from the source, which is called the *primary image*. A second image is taken from the source with the field of view of the imager purposely shifted in the direction represented by the rows of the FPA by at least one pixel (i.e. one instantaneous field of view (IFOV)). This picture is called the *column-shift image*. Finally, a third image is taken with the field of view of the imager purposely shifted in the direction represented by the columns of the FPA by at least one pixel (i.e. one IFOV) in relation to the primary image. This picture is called the *row-shift image*. From these three images the NUC of the imager can be performed. If it is necessary to check the temporal stability of the radiation source and of the imager, during the picture recording process a fourth image can be taken with the field of view of the camera identical to the primary image.

Table 1. Matrix nomenclature used in section 2.1.

Primary image:	P	With the elements $p_{i,j}$
Column-shift image:	S	With the elements $s_{i,j}$
Row-shift image:	Z	With the elements $z_{i,j}$
Column-difference matrix	Q	With the elements $q_{i,j}$
Row-difference matrix	R	With the elements $r_{i,j}$
Result matrix:	E	With the elements $e_{i,j}$

From the primary image and the column-shift image, in each case the difference of the signal values of the two image pixels which look at an identical position of the radiation source is taken. This leads to a column-difference matrix. The same procedure carried out with the primary image and the row-shift image leads to a row-difference matrix. From these two matrices a result matrix is generated which yields the difference between the radiance temperature value of the detector pixels of the FPA and a chosen reference detector pixel of the FPA. This method is called the ***NUC difference method-FPA***.

Another method is that of the primary image and the column-shift image: For each detector pixel the difference in the signal values is taken from the two positions of the radiation source. This leads to a column-difference matrix. The same procedure carried out with the primary image and the row-shift image leads to a row-difference matrix. From these two matrices a result matrix is generated which yields the difference between the radiance temperature value of the radiation source and a chosen reference point on the source. This method is called ***NUC difference-method source***.

Both methods allow the determination of the NUC of the imager (and thereby the determination of the inhomogeneity of the source). The determination of the NUC of the imager requires a conversion of the differences of the radiance temperatures in a change of radiance values, and the reverse, with the help of Planck's formula and it requires an iterative calculation without further new measurements. The appropriate mathematical algorithms are subsequently described in detail. The following designations stated in table 1 are obtained for the calculation.

All images and all matrices with i rows, $i = 1 \ldots n$ and j columns $j = 1 \ldots m$ and n, m are whole numbers.

2.1. Algorithm of NUC difference method-FPA

The image recording system indicates radiance temperature values $t_{\lambda,S}$ for all image points. The following algorithm results in a matrix E^{D} which yields the difference between the radiance temperature values of all individual detector pixels and a chosen reference detector pixel of the imager.

2.1.1. Calculation of column-difference matrix Q. Selection of a reference column Q_j with $j = B$, with B a whole number in the range from $j = 1$ to m, figure 1.

Calculation of the respective differences in the column-difference matrix for all columns $j < B$ according to equation (1):

$$q_{i,j} = s_{i,j} - p_{i,j+1} \text{ for all } q_{i,j} \text{ with } j < B \tag{1}$$

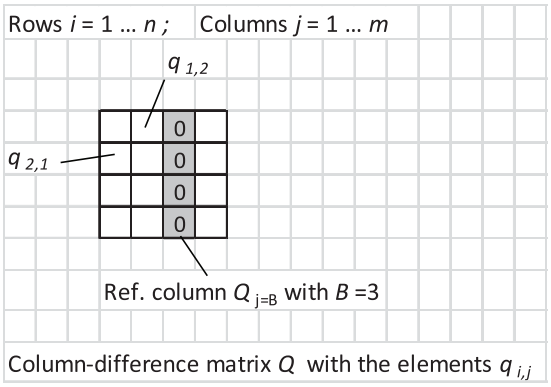

Figure 1. Example of a 4 × 4 column-difference matrix $Q_{i,j}$ with reference column $Q_{i,3}$

Each difference $q_{i,j}$ (of the reference column) for $j = B$ obtains the value 0.

Calculation of the respective difference in the column-difference matrix for all columns $j > B$ according to equation (2)

$$q_{i,j} = p_{i,j} - s_{i,j-1} \text{ for all } q_{i,j} \text{ with } j > B \tag{2}$$

2.1.2. Calculation of row-difference matrix R. Selection of a reference row R_i with $i = b$, with b a whole number in the range from $i = 1$ to n, figure 2.

Calculation of the respective differences in the row-difference matrix for all rows $i < b$ according to equation (3):

$$r_{i,j} = z_{i,j} - p_{i+1,j} \text{ for all } r_{i,j} \text{ with } i < b. \tag{3}$$

Each difference $r_{i,j}$ (of the reference row) for $i = b$ obtains the value 0.

Calculation of the respective difference in the row-quotient matrix for all rows $i > b$ according to equation (4)

$$r_{i,j} = p_{i,j} - z_{i-1,j} \text{ for all } r_{i,j} \text{ with } i > b : \tag{4}$$

2.1.3. Calculation of result matrix E^D. Formation of a reference point of the matrix E^{D} with the value $e_{i=b,j=B} = 0$, figure 3.

y and x are whole numbers.

Calculation of the elements $e_{i,j}$ of the result matrix E^{D}:

for $1 \leqslant y \leqslant m - B$ according to equation (5)

$$e_{i=b,j=B+y} = e_{i=b,j=B+y-1} + q_{i=b,j=B+y} \tag{5}$$

for $1 \leqslant y < B$ according to equation (6)

$$e_{i=b,j=B-y} = e_{i=b,j=B-y+1} + q_{i=b,j=B-y} \tag{6}$$

for $1 \leqslant x \leqslant n - b$ according to equation (7)

$$e_{i=b+x,j=B} = e_{i=b+x-1,j=B} + r_{i=b+x,j=B} \tag{7}$$

for $1 \leqslant x < b$ according to equation (8)

$$e_{i=b-x,j=B} = e_{i=b-x+1,j=B} + r_{i=b-x,j=B} \tag{8}$$

Calculation of the other elements $e_{i,j}$ of the result matrix E^{D}:

For all elements $e_{i,j}$ with $j < B$ and $i < b$ according to equation (9)

$$e_{i,j} = (q_{i,j} + e_{i,j+1} + r_{i,j} + e_{i+1,j})/2 \tag{9}$$

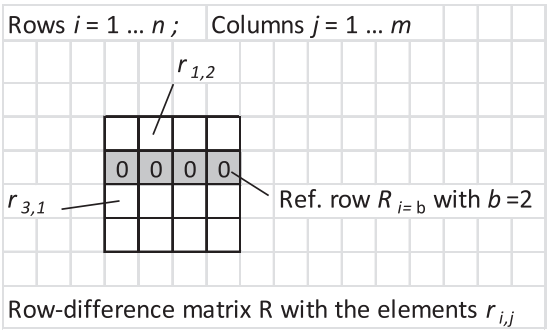

Figure 2. Example of a 4 × 4 row-difference matrix $R_{i,j}$ with reference row $R_{2,j}$.

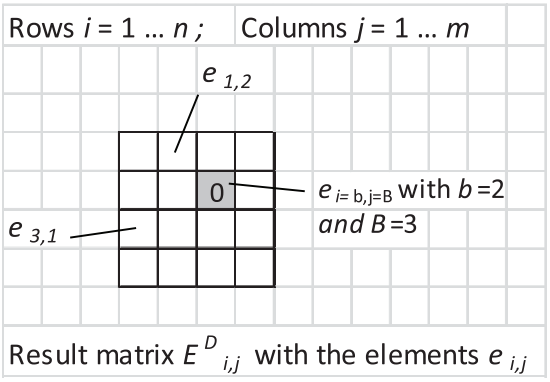

Figure 3. Example of a 4 × 4 result matrix $E^{\mathrm{D}}_{i,j}$ with reference point $E_{2,3}$.

For all elements $e_{i,j}$ with $j < B$ and $i > b$ according to equation (10)

$$e_{i,j} = (q_{i,j} + e_{i,j+1} + r_{i,j} + e_{i-1,j})/2 \tag{10}$$

For all elements $e_{i,j}$ with $j > B$ and $i < b$ according to equation (11)

$$e_{i,j} = (q_{i,j} + e_{i,j-1} + r_{i,j} + e_{i+1,j})/2 \tag{11}$$

For all elements $e_{i,j}$ with $j > B$ and $i > b$ according to equation (12)

$$e_{i,j} = (q_{i,j} + e_{i,j-1} + r_{i,j} + e_{i-1,j})/2 \tag{12}$$

Now the result matrix E^{D} shows the difference in the radiance temperature value of the detector pixels of the FPA relative to the reference point of the result matrix E^{D} (i.e. the reference detector pixel of the FPA: $e_{i=b,j=B} = 0$).

These determined differences in the indicated radiation temperature of the image points of the FPA (or of an image recording system) are, in the case of an inequality of the transmission behavior of the image point of an FPA or of an image recording system, affected by deviations. Therefore, another calculation or several calculations (iterations) are performed after the (re-) determined values of the differences in the radiation temperature of the image point of the FPA or of the image recording system have also been used to correct the inequality of the transmission behavior of the image point of the FPA or of the image recording system.

2.1.4. Calculation of the differences in the determined radiation temperatures of primary image P. Calculation of the difference in the measured radiation temperature due to the inequality of the transmission behavior of the image recording system in a first approximation according to equation (13):

$$d_{i,j} = e_{i,j} \tag{13}$$

Calculation of the matrix $P1$ with the first correction (difference formation) of primary image P according to equation (14):

$$p1_{i,j} = p_{i,j} - d_{i,j} \tag{14}$$

The first correction values (in a first approximation) are now available as the temperature difference for each image point. These values were used to correct primary image P, and the matrix $P1$ was obtained. These correction values are valid only for the radiation temperature determined for each image point. Now these correction values (temperature differences) must be converted into correction factors. This allows the inequality of the transmission behavior of the image recording systems to be corrected (in a first approximation) with validity for another measurement range of the radiation temperature.

2.1.5. Calculation of the correction factors for primary image P, for column-shift image S and for row-shift image Z. The conversion of the correction values into correction factors is performed with the aid of the calculation of the resulting beam densities $L_{\lambda,S}$ as a function of the temperature T (in kelvins) under constant conditions for the respective application of Planck's formula, using a known centroid wavelength λ or a wavelength range (λ_1 to λ_2) of the image recording system.

Planck's formula according to equation (15):

$$L_{\lambda,S} = \frac{c_1}{\pi \cdot \Omega_0} \cdot \frac{1}{\lambda^5} \cdot \frac{1}{e^{c_2/(\lambda \cdot T)} - 1} \text{ with}$$
$$c_1 = 3\,741\,832 \cdot 10^{-16}\ \mathrm{W \cdot m^2}$$
$$c_2 = 1\,438\,786 \cdot 10^{-2}\ \mathrm{m \cdot K}$$
$$\Omega_0 = 1\ \mathrm{sr} \tag{15}$$

For the following calculation, the first two terms of Planck's formula may be omitted, as the respective ratios of the resulting beam densities are formed and the result of the first two terms remains constant during image recording. The following equation (16) is obtained.

$$X_{\lambda,S} = \frac{1}{e^{c_2/(\lambda \cdot T)} - 1} \tag{16}$$

$X_{\lambda,S}$ is a beam-density-proportional value.

Calculation of beam-density-proportional value for primary image P according to equation (17):

$$X_{\lambda,S}(p_{i,j}) = \frac{1}{e^{c_2/\left(\lambda \cdot T(p_{i,j})\right)} - 1} \tag{17}$$

with λ being the centroid wavelength of the image recording system and T (in kelvins) the value of the determined radiation temperature of the respective image point $p_{i,j}$.

Calculation of a beam-density-proportional value for matrix $P1$ (corrected primary image P) according to equation (18):

$$X_{\lambda,S}(p1_{i,j}) = \frac{1}{e^{c_2/\left(\lambda \cdot T(p1_{i,j})\right)} - 1} \tag{18}$$

with λ being the centroid wavelength of the image recording system and T (in kelvins) the value of the radiation temperature of the respective image point $p1_{i,j}$.

Calculation of the first correction factors k_0 (in a first approximation) of the image recording system according to equation (19):

$$k_0(p_{i,j}) = \frac{X_{\lambda,S}(p_{i,j})}{X_{\lambda,S}(p1_{i,j})} \tag{19}$$

The correction factors $k_0(p_{i,j})$ form the correction factor matrix K_0.

Calculation of beam densities (Planck's formula) with values of the radiation temperature T (in kelvins) of the image points of primary image P, the image points of column-shift image S and the image points of row-shift image Z at the known centroid wavelength λ or in a wavelength interval according to equations (20)–(22).

Primary image P:

$$L_{\lambda,S}(p_{i,j}) = \frac{c_1}{\pi \cdot \Omega_0} \cdot \frac{1}{\lambda^5} \cdot \frac{1}{e^{c_2/(\lambda \cdot T(p_{i,j}))} - 1} \tag{20}$$

Column-shift image S:

$$L_{\lambda,S}(s_{i,j}) = \frac{c_1}{\pi \cdot \Omega_0} \cdot \frac{1}{\lambda^5} \cdot \frac{1}{e^{c_2/(\lambda \cdot T(s_{i,j}))} - 1} \tag{21}$$

Row-shift image Z:

$$L_{\lambda,S}(z_{i,j}) = \frac{c_1}{\pi \cdot \Omega_0} \cdot \frac{1}{\lambda^5} \cdot \frac{1}{e^{c_2/(\lambda \cdot T(z_{i,j}))} - 1} \tag{22}$$

The calculated beam densities of the three images P, S, Z are corrected by dividing each calculated beam density with the associated determined correction factor $k_0(p_{i,j})$ (in a first approximation) according to equations (23)–(25):

$$L_{k_1,\lambda,S}(p_{i,j}) = \frac{L_{\lambda,S}(p_{i,j})}{k_0(p_{i,j})} \tag{23}$$

$$L_{k_1,\lambda,S}(s_{i,j}) = \frac{L_{\lambda,S}(s_{i,j})}{k_0(p_{i,j})} \tag{24}$$

$$L_{k_1,\lambda,S}(z_{i,j}) = \frac{L_{\lambda,S}(z_{i,j})}{k_0(p_{i,j})} \tag{25}$$

With the inverse function of Planck's formula, according to equation (26) the resulting corrected radiation temperatures are now calculated from the corrected beam densities for the image points of all three images P, S, Z according to equations (27)–(29).

Inverse, Planck's formula:

$$T_{\lambda,S} = \frac{c_2}{\lambda} \cdot \frac{1}{\ln(c_1 / L_{\lambda,S} \cdot \pi \cdot \Omega_0 \cdot \lambda^5 + 1)} \tag{26}$$

with ($T_{\lambda,S}$ in kelvins)

Primary image P, first correction:

$$T_{k1,\lambda,S}(p_{i,j}) = \frac{c_2}{\lambda} \cdot \frac{1}{\ln\left(c_1/L_{k1,\lambda,S}(p_{i,j}) \cdot \pi \cdot \Omega_0 \cdot \lambda^5 + 1\right)} \quad (27)$$

Column-shift image S, first correction:

$$T_{k1,\lambda,S}(s_{i,j}) = \frac{c_2}{\lambda} \cdot \frac{1}{\ln(c_1/L_{k1,\lambda,S}(s_{i,j}) \cdot \pi \cdot \Omega_0 \cdot \lambda^5 + 1)} \quad (28)$$

Row-shift image Z, first correction:

$$T_{k1,\lambda,S}(z_{i,j}) = \frac{c_2}{\lambda} \cdot \frac{1}{\ln(c_1/L_{k1,\lambda,S}(z_{i,j}) \cdot \pi \cdot \Omega_0 \cdot \lambda^5 + 1)} \quad (29)$$

Three matrices are now available for the three images P, S, Z with the respective corrected values of the (first determined) radiation temperatures for each image point. These matrices are referred to as P_{k1}, S_{k1} and Z_{k1}. The values of matrix P_{k1} are identical with the values of matrix $P1$ (see above).

It must be pointed out that the radiation temperatures $t_{k1,\lambda,S}$ of matrices P_{k1}, S_{k1} and Z_{k1} are (generally) again indicated in the unit °C. Then, the following applies according to equation (30):

$$t_{kn,\lambda,S} = T_{kn,\lambda,S} - 27\,315\,\mathrm{K} \quad (30)$$

The calculated correction factor matrix K_0 with the correction factors indicates the value of the inequality of the transmission behavior of the image points of an FPA or of an image recording system and can be used for correction. If calculation step 2 and other calculation steps are used, new values are obtained for the correction factor matrices K_1, K_2 to K_n with the (new) correction factors $k_1(p_{i,j})$, $k_2(p_{i,j})$ to $k_n(p_{i,j})$, for which values smaller uncertainties can be expected.

2.1.6. Calculation step 2. Now a 1st iteration of calculation step 1 follows, using matrices P_{k1}, S_{k1}, Z_{k1} instead of images P, S, Z. The following designations stated in table 2 are obtained for the 1st iteration.

Calculation of result matrix E^{D}_{k1}. Result matrix E^{D}_{k1} is calculated in accordance with the specifications of point 2.1.3, using, however, matrices P_{k1}, S_{k1} and Z_{k1} for this calculation.

Calculation of the differences in the radiation temperatures of matrix P1. Calculation of the difference in the (corrected) radiation temperature due to the inequality of the transmission behavior of the image recording system according to equation (31):

$$d1_{i,j} = e_{k1,i,j} \quad (31)$$

Calculation of matrix $P2$ with the correction (difference formation) of matrix $P1$ according to equation (32):

$$p2_{i,j} = p1_{i,j} - d1_{i,j} \quad (32)$$

The second correction values are available as temperature difference for each image point. These were used to correct matrix $P1$ and matrix $P2$ was obtained.

A radiation-density-proportional value $X_{\lambda,S}(p_{i,j})$ for primary image P has already been calculated in point 2.1.5.

Calculation of a radiation-density-proportional value for matrix $P2$ according to equation (33):

Table 2. Matrix nomenclature used in section 2.1.6.

Primary image matrix:	P_{k1}
Column-shift image matrix:	S_{k1}
Row-shift image matrix:	Z_{k1}
Column-difference matrix:	Q_{k1}
Row-difference matrix:	R_{k1}
Result matrix:	E_{k1}
Correction factor matrix:	K_1

Table 3. Matrix nomenclature used in section 2.1.7.

Primary image matrix:	P_{k2}
Column-shift image matrix:	S_{k2}
Row-shift image matrix:	Z_{k2}
Column-difference matrix:	Q_{k2}
Row-difference matrix:	R_{k2}
Result matrix:	E_{k2}
Correction factor matrix:	K_2

$$X_{\lambda,S}(p2_{i,j}) = \frac{1}{\mathrm{e}^{c_2/(\lambda \cdot T(p2_{i,j}))} - 1} \quad (33)$$

with λ being the centroid wavelength of the image recording system and T (in kelvins) the value of the radiation temperature of the respective image point $p2_{i,j}$.

Calculation of the new (second) correction factors k_1 of the image recording system according to equation (34):

$$k_1(p_{i,j}) = \frac{X_{\lambda,S}(p_{i,j})}{X_{\lambda,S}\left(p2_{i,j}\right)} \quad (34)$$

The correction factors $k_1(p_{i,j})$ form the correction factor matrix K_1, whereby the correction factor matrix K_0 used so far is replaced.

The calculated correction factor matrix K_1 with the correction factors $k_1(p_{i,j})$ now indicates the (new) value of the inequality of the transmission behavior of the image points of an FPA or of an image recording system and can be used for correction. Compared to correction factor matrix K_0, correction factor matrix K_1 generally shows smaller uncertainties.

Matrices P_{k2}, S_{k2} and Z_{k2} are now calculated as described in point 2.1.5, using, however, correction factor matrix K_1.

2.1.7. Calculation step 3. A 2nd iteration of calculation step 1 can be performed, using matrices P_{k2}, S_{k2}, Z_{k2} instead of images P, S, Z. The matrices have been obtained as the result of calculation step 2. The following designations stated in table 3 are obtained for the 2nd iteration.

Calculation of result matrix E^{D}_{k2}. Result matrix E^{D}_{k2} is calculated in accordance with the specifications of point 2.1.3, using, however, matrices P_{k2}, S_{k2} and Z_{k2} for this calculation.

Calculation of the differences in the radiation temperatures of matrix P2. Calculation of the difference in the (corrected) radiation temperature due to the inequality of the transmission behavior of the image recording system according to equation (35):

$$d2_{i,j} = e_{k2,i,j} \tag{35}$$

Calculation of matrix $P3$ with the correction (difference formation) of matrix $P2$ according to equation (36):

$$p3_{i,j} = p2_{i,j} - d2_{i,j} \tag{36}$$

Now the third correction values are available as temperature difference for each image point. These were used to correct matrix $P2$ and matrix $P3$ was obtained.

A radiation-density-proportional value $X_{\lambda,S}(p_{i,j})$ for primary image P has already been calculated in point 2.1.5.

Calculation of a radiation-density-proportional value for matrix $P3$ according to equation (37):

$$X_{\lambda,S}(p3_{i,j}) = \frac{1}{e^{c_2/(\lambda \cdot T(p3_{i,j}))} - 1} \tag{37}$$

with λ being the centroid wavelength of the image recording system and T (in kelvins) the value of the radiation temperature of the respective image point $p3_{i,j}$.

Calculation of the new (third) correction factors k_2 of the image recording system according to equation (38):

$$k_2(p_{i,j}) = \frac{X_{\lambda,S}(p_{i,j})}{X_{\lambda,S}(p3_{i,j})} \tag{38}$$

The correction factors $k_2(p_{i,j})$ form the correction factor matrix K_2, whereby the correction factor matrix K_1 used so far is replaced.

The calculated correction factor matrix K_2 with the correction factors $k_2(p_{i,j})$ now indicates the (new) value of the inequality of the transmission behavior of the image points of an image recording system which can be used for correction. Compared to the (first and second) correction factor matrices K_0 and K_1, correction factor matrix K_2 generally shows smaller uncertainties.

For further iterations, matrices P_{k3}, S_{k3} and Z_{k3} can now be calculated as described in point 2.1.5. using, however, correction factor matrix K_2.

2.1.8. Calculation steps 4 to n. Further iterations can be performed analog to points 2 and 3. The remaining uncertainty in the practical determination of the uncertainty of the transmission behavior of the image points of an image recording system is also determined by the noise of the image recording system and by short-term instabilities of the components used.

The change in the values of the calculated radiation temperatures of an iteration compared to the values of the measured radiation temperatures, or to the values of the respective calculated radiation temperatures of the previous iteration, is used as a criterion for the termination of the iterations. The limiting value for the change is determined as a function of the uncertainty aimed at. Calculations with 2 iterations may already show very small changes.

2.2. Algorithm of NUC difference method source

The image recording system indicates radiance temperature values $t_{\lambda,S}$ for all image points in degrees Celsius (°C). The following algorithm results in a matrix E^S which yields the

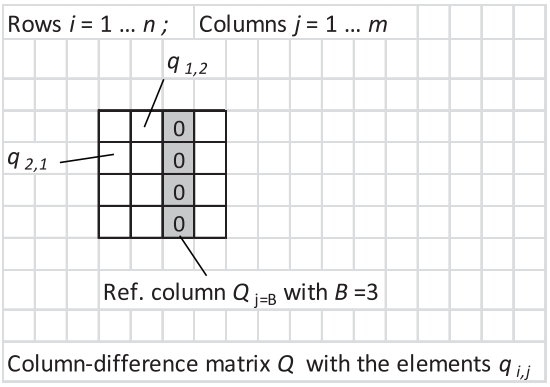

Figure 4. Example of a 4 × 4 column-difference matrix $Q_{i,j}$ with reference column $Q_{i,3}$.

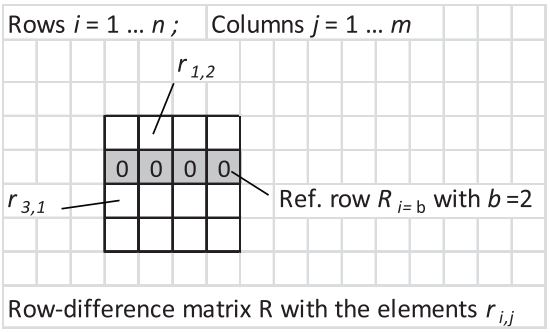

Figure 5. Example of a 4 × 4 row-difference matrix $R_{i,j}$ with reference row $R_{2,j}$.

difference between the radiance temperature value of the radiance of the object points and a chosen reference object point of the source.

2.2.1. Calculation of column-difference matrix Q. Selection of a reference column Q_j with $j = B$, with B a whole number in the range from $j = 1$ to m, figure 4.

Calculation of the respective differences of the column-difference matrix for all columns $j < B$ according to equation (39):

$$q_{i,j} = p_{i,j} - s_{i,j} \text{ for all } q_{i,j} \text{ with } j < B \tag{39}$$

Each difference $q_{i,j}$ (of the reference column) for $j = B$ obtains the value 0.

Calculation of the respective difference of the column-difference matrix for all columns $j > B$ according to equation (40):

$$q_{i,j} = s_{i,j} - p_{i,j} \text{ for all } q_{i,j} \text{ with } j > B \tag{40}$$

2.2.2. Calculation of row-difference matrix R. Selection of a reference row R_i with $i = b$, with b a whole number in the range from $i = 1$ to n, figure 5.

Calculation of the respective differences of the row-difference matrix for all rows $i < b$ according to equation (41):

$$r_{i,j} = p_{i,j} - z_{i,j} \text{ for all } r_{i,j} \text{ with } i < b. \tag{41}$$

Each difference $r_{i,j}$ (of the reference row) for $i = b$ obtains the value 0.

Calculation of the respective difference of the row-quotient matrix for all rows $i > b$ according to equation (42):

$$r_{i,j} = z_{i,j} - p_{i,j} \text{ for all } r_{i,j} \text{ with } i > b \tag{42}$$

2.2.3. Calculation of result matrix E^S. Formation of a reference point of the matrix E^S with the value $e_{i=b,j=B} = 0$, figure 6.

y and x are whole numbers.

Calculation of the elements $e_{i,j}$ of the result matrix E^S:
for $1 \leqslant y \leqslant m - B$ according to equation (43)

$$e_{i=b,j=B+y} = e_{i=b,j=B+y-1} + q_{i=b,j=B+y} \tag{43}$$

for $1 \leqslant y < B$ according to equation (44)

$$e_{i=b,j=B-y} = e_{i=b,j=B-y+1} + q_{i=b,j=B-y} \tag{44}$$

for $1 \leqslant x \leqslant n - b$ according to equation (45)

$$e_{i=b+x,j=B} = e_{i=b+x-1,j=B} + r_{i=b+x,j=B} \tag{45}$$

for $1 \leqslant x < b$ according to equation (46)

$$e_{i=b-x,j=B} = e_{i=b-x+1,j=B} + r_{i=b-x,j=B} \tag{46}$$

Calculation of the other elements $e_{i,j}$ of the result matrix E^S:

For all elements $e_{i,j}$ with $j < B$ and $i < b$ according to equation (47)

$$e_{i,j} = (q_{i,j} + e_{i,j+1} + r_{i,j} + e_{i+1,j})/2 \tag{47}$$

For all elements $e_{i,j}$ with $j < B$ and $i > b$ according to equation (48)

$$e_{i,j} = (q_{i,j} + e_{i,j+1} + r_{i,j} + e_{i-1,j})/2 \tag{48}$$

For all elements $e_{i,j}$ with $j > B$ and $i < b$ according to equation (49)

$$e_{i,j} = (q_{i,j} + e_{i,j-1} + r_{i,j} + e_{i+1,j})/2 \tag{49}$$

For all elements $e_{i,j}$ with $j > B$ and $i > b$ according to equation (50)

$$e_{i,j} = (q_{i,j} + e_{i,j-1} + r_{i,j} + e_{i-1,j})/2 \tag{50}$$

Now the result matrix E^S shows the differences in the measured radiance temperature values of the object points of the source related to the reference point of the result matrix E^S.

These determined differences in the indicated radiation temperature of the object points of the source are, in the case of an inequality of the transmission behavior of the image point of an image recording system, affected by deviations. Therefore, another calculation or several calculations (iterations) are performed after the (re-) determined values of the differences of the radiation temperature of the object points have been used to correct the inequality of the transmission behavior of the image points of the imaging recording system.

2.2.4. Calculation of the differences in the determined radiance temperatures of primary image P. Differences to the reference point according to equation (51):

$$\Delta p_{i,j} = p_{i,j} - p_{i=b,j=B} \tag{51}$$

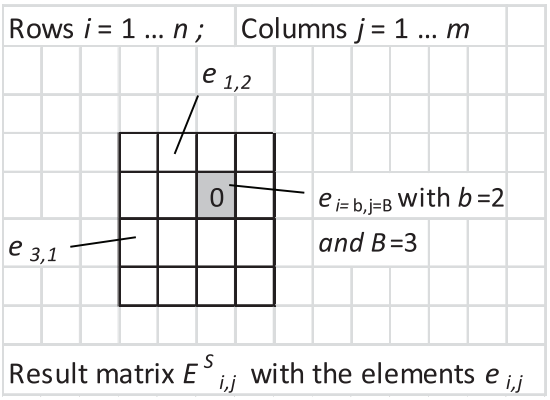

Figure 6. Example of a 4 × 4 result matrix $E^S_{i,j}$ with reference point $E_{2,3}$.

Calculation of the difference in the measured radiance temperature due to the inequality of the transmission behavior of the image recording system in the first approximation according to equation (52):

$$d_{i,j} = \Delta p_{i,j} - e_{i,j} \tag{52}$$

Calculation of the matrix $P1$ with the first correction (difference formation) of primary image P according to equation (53):

$$p1_{i,j} = p_{i,j} - d_{i,j} \tag{53}$$

The first correction values (in the first approximation) are now available as temperature difference for each image point. These values were used to correct primary image P, and the matrix $P1$ was obtained. These correction values are valid only for the radiation temperature determined for each image point. Now these correction values (temperature differences) must be converted into correction factors. This allows the inequality of the transmission behavior of the image recording systems to be corrected (in the first approximation) with validity for another measurement range of the radiation temperature.

2.2.5. Calculation of the correction factors for primary image P, for column-shift image S and for row-shift image Z. The conversion of the correction values into correction factors is performed with the aid of the calculation of the resulting beam densities $L_{\lambda,S}$ as a function of the temperature T (in kelvins) under constant conditions for the respective application of Planck's formula, using a known centroid wavelength λ or a wavelength range (λ_1 to λ_2) of the image recording system.

Planck's formula according to equation (54):

$$L_{\lambda,S} = \frac{c_1}{\pi \cdot \Omega_0} \cdot \frac{1}{\lambda^5} \cdot \frac{1}{e^{c_2/(\lambda \cdot T)} - 1} \text{ with}$$
$$c_1 = 3\,741\,832 \cdot 10^{-16}\ \mathrm{W \cdot m^2}$$
$$c_2 = 1\,438\,786 \cdot 10^{-2}\ \mathrm{m \cdot K}$$
$$\Omega_0 = 1\ \mathrm{sr} \tag{54}$$

For the following calculation, the first two terms of Planck's formula may be omitted, as the respective ratios of the resulting beam densities are formed and the result of the first two terms remains constant during image recording. Equation (55) is obtained as follows:

$$X_{\lambda,S} = \frac{1}{e^{c_2/(\lambda \cdot T)} - 1} \tag{55}$$

$X_{\lambda,S}$ is a beam-density-proportional value.

Calculation of beam-density-proportional value for primary image P according to equation (56):

$$X_{\lambda,S}(p_{i,j}) = \frac{1}{e^{c_2/\left(\lambda \cdot T(p_{i,j})\right)} - 1} \tag{56}$$

with λ being the centroid wavelength of the image recording system and T (in kelvins) the value of the determined radiation temperature of the respective image point $p_{i,j}$.

Calculation of a beam-density-proportional value for matrix $P1$ (corrected primary image P) according to equation (57):

$$X_{\lambda,S}(p1_{i,j}) = \frac{1}{e^{c_2/(\lambda \cdot T(p1_{i,j}))} - 1} \tag{57}$$

with λ being the centroid wavelength of the image recording system and T (in kelvins) the value of the radiation temperature of the respective image point $p1_{i,j}$.

Calculation of the first correction factors k_0 (in the first approximation) of the image recording system according to equation (58):

$$k_0(p_{i,j}) = \frac{X_{\lambda,S}(p_{i,j})}{X_{\lambda,S}\left(p1_{i,j}\right)} \tag{58}$$

The correction factors $k_0(p_{i,j})$ form the correction factor matrix K_0.

Calculation of beam densities (Planck's formula) with values of the radiation temperature T (in kelvins) of the image points of primary image P, the image points of column-shift image S and the image points of row-shift image Z at the known centroid wavelength λ or in a wavelength interval according to equations (59)–(61).

Primary image P:

$$L_{\lambda,S}(p_{i,j}) = \frac{c_1}{\pi \cdot \Omega_0} \cdot \frac{1}{\lambda^5} \cdot \frac{1}{e^{c_2/\left(\lambda \cdot T(p_{i,j})\right)} - 1} \tag{59}$$

Column-shift image S:

$$L_{\lambda,S}(s_{i,j}) = \frac{c_1}{\pi \cdot \Omega_0} \cdot \frac{1}{\lambda^5} \cdot \frac{1}{e^{c_2/(\lambda \cdot T(s_{i,j}))} - 1} \tag{60}$$

Row-shift image Z:

$$L_{\lambda,S}(z_{i,j}) = \frac{c_1}{\pi \cdot \Omega_0} \cdot \frac{1}{\lambda^5} \cdot \frac{1}{e^{c_2/(\lambda \cdot T(z_{i,j}))} - 1} \tag{61}$$

The calculated beam densities of the three images P, S, Z are corrected by dividing each calculated beam density by the associated determined correction factor $k_0(p_{i,j})$ (in the first approximation) according to equations (62)–(64).

$$L_{k_1,\lambda,S}(p_{i,j}) = \frac{L_{\lambda,S}(p_{i,j})}{k_0(p_{i,j})} \tag{62}$$

$$L_{k_1,\lambda,S}(s_{i,j}) = \frac{L_{\lambda,S}(s_{i,j})}{k_0(p_{i,j})} \tag{63}$$

$$L_{k_1,\lambda,S}(z_{i,j}) = \frac{L_{\lambda,S}(z_{i,j})}{k_0(p_{i,j})} \tag{64}$$

With the inverse function of Planck's formula, according to equation (65) the resulting corrected radiation temperatures are now calculated from the corrected beam densities for the image points of all three images P, S, Z according to equations (66)–(68).

Inverse, Planck's formula:

$$T_{\lambda,S} = \frac{c_2}{\lambda} \cdot \frac{1}{\ln(c_1/L_{\lambda,S} \cdot \pi \cdot \Omega_0 \cdot \lambda^5 + 1)} \tag{65}$$

with ($T_{\lambda,S}$ in kelvins)

Primary image P, first correction:

$$T_{k1,\lambda,S}(p_{i,j}) = \frac{c_2}{\lambda} \cdot \frac{1}{\ln\left(c_1/L_{k1,\lambda,S}(p_{i,j}) \cdot \pi \cdot \Omega_0 \cdot \lambda^5 + 1\right)} \tag{66}$$

Column-shift image S, first correction:

$$T_{k1,\lambda,S}(s_{i,j}) = \frac{c_2}{\lambda} \cdot \frac{1}{\ln(c_1/L_{k1,\lambda,S}(s_{i,j}) \cdot \pi \cdot \Omega_0 \cdot \lambda^5 + 1)} \tag{67}$$

Row-shift image Z, first correction:

$$T_{k1,\lambda,S}(z_{i,j}) = \frac{c_2}{\lambda} \cdot \frac{1}{\ln(c_1/L_{k1,\lambda,S}(z_{i,j}) \cdot \pi \cdot \Omega_0 \cdot \lambda^5 + 1)} \tag{68}$$

Three matrices are now available for the three images P, S, Z, with the respective corrected values of the (first determined) radiation temperatures for each image point. These matrices are referred to as P_{k1}, S_{k1} and Z_{k1}. The values of matrix P_{k1} are identical with the values of matrix $P1$ (see above).

It must be pointed out that the radiation temperatures $t_{k1,\lambda,S}$ of matrices P_{k1}, S_{k1} and Z_{k1} are (generally) again indicated in the unit °C. Then, the following applies according to equation (69):

$$t_{kn,\lambda,S} = T_{kn,\lambda,S} - 27\,315\,\mathrm{K} \tag{69}$$

The calculated correction factor matrix K_0 with the correction factors indicates the value of the inequality of the transmission behavior of the image points of an FPA or of an image recording system and can be used for correction. If calculation step 2 and other calculation steps are used, new values are obtained for the correction factor matrices K_1, K_2 to K_n with the (new) correction factors $k_1(p_{i,j})$, $k_2(p_{i,j})$ to $k_n(p_{i,j})$, for which values smaller uncertainties can be expected.

2.2.6. Calculation step 2. Now a 1st iteration of calculation step 1 follows, using matrices P_{k1}, S_{k1}, Z_{k1} instead of images P, S, Z. The following designations stated in table 4 are obtained for the 1st iteration.

Calculation of result matrix E^{S}_{k1}. Result matrix E^{S}_{k1} is calculated in accordance with the specifications of point 2.2.3, using, however, matrices P_{k1}, S_{k1} and Z_{k1} for this calculation.

Calculation of the differences in the radiation temperatures of matrix P1. Calculation of the difference in the (corrected) radiation temperature due to the inequality of the transmission behavior of the image recording system according to equation (70):

$$d1_{i,j} = \Delta p_{i,j} - e_{k1,i,j} \tag{70}$$

Table 4. Matrix nomenclature used in section 2.2.6.

Primary image matrix:	P_{k1}
Column-shift image matrix:	S_{k1}
Row-shift image matrix:	Z_{k1}
Column-difference matrix:	Q_{k1}
Row-difference matrix:	R_{k1}
Result matrix:	E_{k1}
Correction factor matrix:	K_1

Calculation of matrix $P2$ with the correction (difference formation) of matrix $P1$ according to equation (71):

$$p2_{i,j} = p1_{i,j} - d1_{i,j} \tag{71}$$

The second correction values are available as temperature difference for each image point. These were used to correct matrix $P1$ and matrix $P2$ was obtained.

A radiation-density-proportional value $X_{\lambda,S}(p_{i,j})$ for primary image P has already been calculated in point 2.2.5.

Calculation of a radiation-density-proportional value for matrix $P2$ according to equation (72):

$$X_{\lambda,S}(p2_{i,j}) = \frac{1}{e^{c_2/(\lambda \cdot T(p2_{i,j}))} - 1} \tag{72}$$

with λ being the centroid wavelength of the image recording system and T (in kelvins) the value of the radiation temperature of the respective image point $p2_{i,j}$.

Calculation of the new (second) correction factors k_1 of the image recording system according to equation (73):

$$k_1(p_{i,j}) = \frac{X_{\lambda,S}(p_{i,j})}{X_{\lambda,S}(p2_{i,j})} \tag{73}$$

The correction factors $k_1(p_{i,j})$ form the correction factor matrix K_1, whereby the correction factor matrix K_0 used so far is replaced.

The calculated correction factor matrix K_1 with the correction factors $k_1(p_{i,j})$ now indicates the (new) value of the inequality of the transmission behavior of the image points of an FPA or of an image recording system and can be used for correction. Compared to correction factor matrix K_0, correction factor matrix K_1 generally shows smaller uncertainties.

Matrices P_{k2}, S_{k2} and Z_{k2} are now calculated as described in point 2.2.5, using, however, correction factor matrix K_1.

2.2.7. Calculation step 3. A 2nd iteration of calculation step 1 can be performed using matrices P_{k2}, S_{k2}, Z_{k2} instead of images P, S, Z. The matrices have been obtained as the result of calculation step 2. The following designations stated in table 5 are obtained for the 2nd iteration.

Calculation of result matrix E^{S}_{k2}. Result matrix E^{S}_{k2} is calculated in accordance with the specifications of point 2.2.3, using, however, matrices P_{k2}, S_{k2} and Z_{k2} for this calculation.

Calculation of the differences in the radiation temperatures of matrix P2. Calculation of the difference in the (corrected) radiation temperature due to the inequality of the transmission behavior of the image recording system according to equation (74):

Table 5. Matrix nomenclature used in section 2.2.7.

Primary image matrix:	P_{k2}
Column-shift image matrix:	S_{k2}
Row-shift image matrix:	Z_{k2}
Column-difference matrix:	Q_{k2}
Row-difference matrix:	R_{k2}
Result matrix:	E_{k2}
Correction factor matrix:	K_2

$$d2_{i,j} = \Delta p_{i,j} - e_{k2,i,j} \tag{74}$$

Calculation of matrix $P3$ with the correction (difference formation) of matrix $P2$ according to equation (75):

$$p3_{i,j} = p2_{i,j} - d2_{i,j} \tag{75}$$

Now the third correction values are available as temperature difference for each image point. These were used to correct matrix $P2$ and matrix $P3$ was obtained.

A radiation-density-proportional value $X_{\lambda,S}(p_{i,j})$ for primary image P has already been calculated in point 2.2.5.

Calculation of a radiation-density-proportional value for matrix $P3$ according to equation (76):

$$X_{\lambda,S}(p3_{i,j}) = \frac{1}{e^{c_2/(\lambda \cdot T(p3_{i,j}))} - 1} \tag{76}$$

with λ being the centroid wavelength of the image recording system and T (in kelvins) the value of the radiation temperature of the respective image point $p3_{i,j}$.

Calculation of the new (third) correction factors k_2 of the image recording system according to equation (77):

$$k_2(p_{i,j}) = \frac{X_{\lambda,S}(p_{i,j})}{X_{\lambda,S}(p3_{i,j})} \tag{77}$$

The correction factors $k_2(p_{i,j})$ form the correction factor matrix K_2, whereby the correction factor matrix K_1 used so far is replaced.

The calculated correction factor matrix K_2 with the correction factors $k_2(p_{i,j})$ now indicates the (new) value of the inequality of the transmission behavior of the image points of an image recording system which can be used for correction. Compared to the (first and second) correction factor matrices K_0 and K_1, correction factor matrix K_2 generally shows smaller uncertainties.

For further iterations, matrices P_{k3}, S_{k3} and Z_{k3} can now be calculated as described in point 2.2.5, using, however, correction factor matrix K_2.

2.2.8. Calculation steps 4 to n. Further iterations can be performed analog to points 2 and 3. The remaining uncertainty in the practical determination of the uncertainty of the transmission behavior of the image points of an image recording system is also determined by the noise of the image recording system and by short-term instabilities of the components used.

The change in the values of the calculated radiation temperatures of an iteration compared to the values of the measured radiation temperatures, or to the values of the respective calculated radiation temperatures of the previous iteration, is

Table 6. 8 × 8 matrix describing an arbitrary radiance temperature distribution in degrees Celsius of a source.

100.00	102.00	103.00	101.00	103.00	105.00	99.00	104.00
101.00	100.50	105.00	99.50	105.00	101.00	103.00	105.00
99.00	101.00	103.00	100.00	98.50	105.00	102.00	101.00
102.00	100.00	102.00	104.00	105.00	101.00	99.00	97.00
98.00	101.00	102.50	105.00	110.00	108.00	105.00	101.00
102.00	100.00	99.00	95.50	105.00	102.00	99.00	98.00
100.00	97.00	101.00	105.00	97.00	101.00	100.00	103.00
95.00	100.00	80.00	101.00	103.00	105.00	102.00	75.00

Table 7. 8 × 8 matrix describing an arbitrary response distribution of the 8 × 8 pixels of an FPA.

50.00	22.00	11.00	88.00	55.00	99.00	8.00	42.00
18.00	56.00	33.00	56.00	33.00	23.00	22.00	23.00
15.00	77.00	46.00	33.00	59.00	48.00	37.00	38.00
33.00	14.00	88.00	41.00	72.00	42.00	15.00	27.00
59.00	43.00	51.00	15.00	33.00	36.00	64.00	66.00
6.00	22.00	29.00	26.00	15.00	73.00	77.00	23.00
88.00	56.00	16.00	75.00	48.00	64.00	17.00	85.00
33.00	12.00	55.00	56.00	99.00	23.00	56.00	60.00

Table 8. Response distribution of the 8 × 8 pixels of the FPA given in table 7 normalized to the pixel response in column 5 and row 5 (user-defined reference pixel).

1.515	0.667	0.333	2.667	1.667	3.000	0.242	1.273
0.545	1.697	1.000	1.697	1.000	0.697	0.667	0.697
0.455	2.333	1.394	1.000	1.788	1.455	1.121	1.152
1.000	0.424	2.667	1.242	2.182	1.273	0.455	0.818
1.788	1.303	1.545	0.455	1.000	1.091	1.939	2.000
0.182	0.667	0.879	0.788	0.455	2.212	2.333	0.697
2.667	1.697	0.485	2.273	1.455	1.939	0.515	2.576
1.000	0.364	1.667	1.697	3.000	0.697	1.697	1.818

Table 9. 8 × 8 matrix describing the primary image (P) as a result of tables 6 and 8, values in degrees Celsius.

121.24	83.17	55.78	155.64	129.90	168.74	41.37	116.30
73.68	128.03	105.00	126.88	105.00	84.23	84.07	87.88
64.57	147.28	120.06	100.00	128.63	124.57	107.68	107.99
102.00	62.67	156.95	115.04	148.16	113.11	64.57	87.69
128.05	114.33	125.12	69.51	110.00	112.44	141.03	138.03
33.80	81.37	92.89	84.58	69.51	145.28	144.76	81.49
154.33	124.00	68.82	150.69	115.73	136.23	70.46	156.04
95.00	56.74	103.61	128.61	166.01	87.88	129.76	102.13

used as a criterion for the termination of the iterations. The limiting value for the change is determined as a function of the uncertainty aimed at. Calculations with two iterations may already show very small changes.

3. Numerical simulation of the NUC method

We present a calculation example of the NUC methods which have been introduced in section 2.1. This exemplification illustrates the NUC difference method-FPA. For this purpose, two 8 × 8 matrices are set up with arbitrarily chosen values. One matrix describes the spatially inhomogeneous radiance temperature distribution of a temporarily stable source. The other matrix describes the values of the response characteristics of the pixels, a nonhomogeneous FPA. Although the numerical values have been arbitrarily chosen, the scatter of these values has been chosen in such a way that they represent typical practical radiance temperatures and responsivity distributions of nonhomogeneous sources, and FPAs applied for the NUC. Starting from the matrix describing the radiance temperature distribution of the source we show that the method leads to a correction factor matrix which describes the predetermined values of the response characteristics of the 8 × 8 pixels of the FPA with a very small remaining relative deviation of generally less than 1×10^{-4} after two iteration processes according to table 22.

3.1. Numerical simulation of the algorithm of NUC difference method-FPA

In table 6, an arbitrarily chosen radiance temperature distribution in degrees Celsius (°C) of a conceived radiation source is given by an 8 × 8 matrix. In table 7, an arbitrarily chosen

Table 10. 8 × 8 matrix describing the column-shift image (S) as a result of tables 6 and 8, values in degrees Celsius. The imager was shifted in the direction represented by the rows of the FPA by 1 pixel (i.e. 1 IFOV).

123.47	84.07	54.25	158.27	132.19	160.57	44.94	#DIV/0!
73.25	133.22	99.50	133.22	101.00	86.06	85.88	#DIV/0!
66.22	149.81	116.79	98.50	136.24	121.26	106.65	#DIV/0!
100.00	64.29	159.58	116.10	143.20	110.97	62.93	#DIV/0!
131.56	115.94	127.93	73.61	108.00	109.37	136.23	#DIV/0!
32.46	80.46	89.50	93.52	67.04	141.55	143.50	#DIV/0!
150.40	128.61	72.16	140.67	120.15	135.04	73.00	#DIV/0!
100.00	41.01	127.60	130.91	168.74	85.14	98.79	#DIV/0!

Table 11. 8 × 8 matrix describing the row-shift image (Z) as a result of tables 6 and 8, values in degrees Celsius. The imager was shifted in the direction represented by the columns of the FPA by 1 pixel (i.e. 1 IFOV).

122.36	81.82	57.31	153.67	132.19	163.29	44.23	117.37
71.96	128.61	103.00	127.46	98.50	87.88	83.17	84.23
67.04	146.02	118.97	104.00	136.24	120.15	104.59	103.84
98.00	63.48	157.61	116.10	154.37	120.57	69.51	91.49
132.72	113.26	121.19	61.69	105.00	106.30	133.84	134.41
32.46	78.66	94.82	93.52	62.93	144.04	146.02	86.06
147.78	127.46	51.19	145.68	122.36	141.03	72.15	119.98
#DIV/0!	#DIV/0!	#DIV/0!	#DIV/0!	#DIV/0!	#DIV/0!	#DIV/0!	#DIV/0!

Table 12. The column-difference matrix (Q) as a result of the primary image (table 9) and the column-shift image (table 10).

40.30	28.30	−101.39	28.37	0.00	36.55	−119.20	71.36
−54.79	28.22	−27.38	28.22	0.00	−16.77	−1.98	2.00
−81.06	29.75	16.79	−30.13	0.00	−11.67	−13.58	1.34
37.33	−92.66	44.54	−32.06	0.00	−30.10	−46.40	24.76
17.23	−9.18	58.42	−36.39	0.00	4.44	31.65	1.80
−48.91	−12.42	4.92	24.01	0.00	78.24	3.21	−62.01
26.40	59.79	−78.53	24.94	0.00	16.08	−64.58	83.04
43.26	−62.60	−1.01	−35.10	0.00	−80.86	44.62	3.35

Table 13. The row-difference matrix (R) as a result of the primary image (table 9) and the row-shift image (table 11).

48.68	−46.21	−47.69	26.79	27.19	79.06	−39.85	29.49
7.38	−18.68	−17.06	27.46	−30.13	−36.69	−24.51	−23.76
−34.96	83.35	−37.98	−11.04	−11.92	7.05	40.01	16.15
−30.05	−50.85	32.49	46.59	44.37	8.13	−71.52	−46.54
0.00	0.00	0.00	0.00	0.00	0.00	0.00	0.00
−98.93	−31.89	−28.30	22.89	−35.49	38.98	10.92	−52.92
121.87	45.34	−26.00	57.17	52.81	−7.80	−75.57	69.98
−52.78	−70.72	52.42	−17.07	43.65	−53.15	57.61	−17.85

Table 14. The result matrix (E^{D}) as a result of the column-difference matrix (table 12) and the row-difference matrix (table 13).

22.48	−17.23	−45.27	57.15	29.51	64.93	−55.89	14.49
−26.78	28.72	1.40	29.63	2.32	−15.26	−17.66	−15.99
−34.87	46.48	17.61	1.27	32.45	20.63	6.43	7.44
−0.20	−37.75	55.16	11.25	44.37	13.42	−34.20	−9.04
30.08	12.85	22.03	−36.39	0.00	4.44	36.10	37.89
−68.48	−19.19	−6.92	−12.49	−35.49	43.08	46.65	−15.19
52.88	25.97	−33.99	43.47	17.32	34.34	−29.58	54.13
0.29	−42.78	21.78	26.14	60.97	−19.35	26.65	33.14

Table 15. The corrected primary image matrix ($P1$) as a result of the primary image (table 9) and the result matrix (E^{D}) (table 14).

98.75	100.41	101.04	98.49	100.39	103.81	97.26	101.81
100.45	99.32	103.60	97.25	102.68	99.49	101.73	103.87
99.44	100.80	102.45	98.73	96.18	103.95	101.25	100.55
102.20	100.42	101.79	103.78	103.79	99.68	98.77	96.73
97.97	101.48	103.09	105.90	110.00	108.00	104.93	100.14
102.27	100.56	99.81	97.07	105.00	102.20	98.11	96.68
101.44	98.03	102.81	107.22	98.42	101.89	100.03	101.91
94.71	99.52	81.83	102.47	105.04	107.23	103.11	69.00

Table 16. The correction factor matrix K_0 as a result of the result matrix (E^{D}) (table 14) and the calculation of section 2.1.5.

1.555	0.689	0.347	2.809	1.758	3.073	0.251	1.331
0.552	1.739	1.029	1.779	1.048	0.719	0.684	0.713
0.450	2.343	1.410	1.027	1.877	1.486	1.139	1.162
0.996	0.421	2.678	1.248	2.236	1.308	0.457	0.823
1.789	1.290	1.527	0.446	1.000	1.091	1.942	2.036
0.181	0.659	0.864	0.762	0.455	2.203	2.377	0.716
2.588	1.661	0.467	2.174	1.412	1.904	0.515	2.634
1.006	0.367	1.598	1.647	2.878	0.667	1.659	2.102

Table 17. The result matrix (E^{D}_{k1}) as result of the 1st iteration according to section 2.1.6.

−1.27	−1.63	−2.01	−2.59	−2.68	−1.23	−1.82	−2.22
−0.55	−1.21	−1.43	−2.34	−2.35	−1.58	−1.31	−1.15
0.46	−0.20	−0.57	−1.33	−2.43	−1.09	−0.79	−0.48
0.23	0.45	−0.20	−0.22	−1.24	−1.37	−0.26	−0.29
0.01	0.51	0.62	0.92	0.00	0.00	−0.07	−0.86
0.31	0.60	0.86	1.64	0.00	0.20	−0.89	−1.33
1.48	1.07	1.83	2.17	1.42	0.88	0.03	−1.08
−0.19	−0.33	2.04	1.45	2.00	2.18	1.10	−6.00

Table 18. The corrected primary image matrix ($P2$) as a result of the primary image (table 9) and the result matrix (E^{D}_{k1}) (table 16).

100.03	102.04	103.05	101.08	103.06	105.04	99.08	104.03
101.00	100.53	105.03	99.59	105.03	101.07	103.04	105.02
98.98	101.00	103.02	100.07	98.61	105.03	102.04	101.03
101.97	99.97	101.99	104.01	105.03	101.05	99.04	97.02
97.96	100.96	102.47	104.98	110.00	108.00	105.00	101.00
101.96	99.96	98.95	95.42	105.00	102.00	99.00	98.01
99.97	96.95	100.98	105.05	97.00	101.01	100.00	102.99
94.90	99.86	79.79	101.02	103.05	105.05	102.01	75.00

Table 19. The correction factor matrix $K1$ as a result of the result matrix (E^{D}_{k1}) (table 16) and the calculation of section 2.1.6.

1.514	0.666	0.333	2.662	1.665	2.997	0.242	1.272
0.545	1.696	0.999	1.694	0.999	0.696	0.666	0.697
0.455	2.333	1.393	0.999	1.784	1.454	1.120	1.151
1.001	0.424	2.667	1.242	2.180	1.271	0.454	0.818
1.789	1.304	1.546	0.455	1.000	1.091	1.939	2.000
0.182	0.667	0.880	0.789	0.455	2.212	2.333	0.697
2.668	1.699	0.485	2.270	1.455	1.939	0.515	2.576
1.002	0.365	1.675	1.696	2.997	0.696	1.697	1.818

Table 20. The result matrix (E^{D}_{k2}) as result of the 2nd iteration according to section 2.1.7.

0.031	0.041	0.057	0.083	0.067	0.045	0.084	0.033
0.001	0.030	0.030	0.092	0.039	0.077	0.046	0.018
−0.022	−0.002	0.023	0.071	0.118	0.033	0.038	0.029
−0.029	−0.028	−0.012	0.005	0.033	0.055	0.039	0.025
−0.037	−0.037	−0.033	−0.025	0.000	0.000	0.000	0.001
−0.039	−0.045	−0.053	−0.078	0.000	0.000	0.000	0.010
−0.033	−0.047	−0.017	0.049	0.000	0.015	0.002	−0.012
−0.106	−0.145	−0.225	0.017	0.046	0.051	0.010	0.000

Table 21. The 3rd primary image matrix ($P3$) as a result of the primary image (table 9) and the result matrix (E^{D}_{k2}) (table 19).

100.00	102.00	103.00	101.00	103.00	105.00	99.00	104.00
101.00	100.50	105.00	99.50	105.00	101.00	103.00	105.00
99.00	101.00	103.00	100.00	98.50	105.00	102.00	101.00
102.00	100.00	102.00	104.00	105.00	101.00	99.00	97.00
98.00	101.00	102.50	105.00	110.00	108.00	105.00	101.00
102.00	100.00	99.00	95.50	105.00	102.00	99.00	98.00
100.00	97.00	101.00	105.00	97.00	101.00	100.00	103.00
95.00	100.00	80.01	101.00	103.00	105.00	102.00	75.00

Table 22. The correction factor matrix $K2$ as a result of the result matrix (E^{D}_{k2}) (table 19) of the 2nd iteration and the calculation of section 2.1.7.

1.515	0.667	0.333	2.667	1.667	3.000	0.242	1.273
0.545	1.697	1.000	1.697	1.000	0.697	0.667	0.697
0.455	2.333	1.394	1.000	1.788	1.455	1.121	1.152
1.000	0.424	2.667	1.242	2.182	1.273	0.455	0.818
1.788	1.303	1.545	0.455	1.000	1.091	1.939	2.000
0.182	0.667	0.879	0.788	0.455	2.212	2.333	0.697
2.667	1.697	0.485	2.273	1.455	1.939	0.515	2.576
1.000	0.364	1.666	1.697	3.000	0.697	1.697	1.818

Table 23. Resulting relative deviation of the determined nonhomogeneity to the given nonhomogeneity (of the example) after the 2nd iteration.

3×10^{-5}	5×10^{-5}	7×10^{-5}	1×10^{-4}	9×10^{-5}	6×10^{-5}	8×10^{-5}	3×10^{-5}
6×10^{-6}	3×10^{-5}	5×10^{-5}	1×10^{-4}	7×10^{-5}	7×10^{-5}	4×10^{-5}	2×10^{-5}
-2×10^{-5}	-2×10^{-6}	2×10^{-5}	6×10^{-5}	1×10^{-4}	2×10^{-5}	3×10^{-5}	2×10^{-5}
-2×10^{-5}	-2×10^{-5}	-1×10^{-5}	3×10^{-6}	2×10^{-5}	4×10^{-5}	4×10^{-5}	3×10^{-5}
-4×10^{-5}	-3×10^{-5}	-2×10^{-5}	-1×10^{-5}	0×10^{0}	0×10^{0}	-1×10^{-16}	3×10^{-12}
-2×10^{-5}	-3×10^{-5}	-4×10^{-5}	-6×10^{-5}	2×10^{-15}	2×10^{-15}	-1×10^{-12}	2×10^{-7}
-3×10^{-5}	-4×10^{-5}	-2×10^{-5}	-1×10^{-5}	1×10^{-15}	3×10^{-11}	8×10^{-7}	-3×10^{-6}
-6×10^{-5}	-4×10^{-6}	-3×10^{-4}	7×10^{-6}	1×10^{-10}	-8×10^{-6}	4×10^{-6}	-3×10^{-6}

response distribution of the 8 × 8 pixels of a conceived FPA is given. Table 8 is generated from table 7 by normalizing all pixel responses to the response of the pixel in column 5 and row 5 (user-defined reference pixel). Table 9 is an 8 × 8 matrix describing the primary image (P). It results from two pixel by pixel calculations with the aid of Planck's formula (and the reverse Planck's formula) at a center wavelength of 5 μm of table 6 (radiance temperature of source) and table 8 (normalized response distribution of FPA). All calculations with help of the Planck formula have used a center wavelength of 5 μm for this simulation. Table 10 is an 8 × 8 matrix describing the column-shift image (S) as a result of tables 6 and 8. The imager was shifted in the direction represented by the rows of the FPA by 1 pixel (i.e. 1 IFOV). Table 11 is an 8 × 8 matrix describing the row-shift image (Z) as a result of tables 6 and 9. The imager was shifted in the direction represented by the columns of the FPA by 1 pixel (i.e. 1 IFOV).

Table 12 is an 8 × 8 matrix describing the column-difference matrix (Q) as a result of tables 9 and 10. Table 12 is calculated according to equations (1) and (2). Table 13 is an 8 × 8 matrix describing the row-quotient matrix (R) as a result of tables 9 and 11. Table 13 is calculated according to equations (3) and (4). Table 14 is an 8 × 8 matrix describing the result matrix (E^{D}) as a result of tables 12 and 13. Table 14 is calculated according to equations (5)–(12). Table 15 is the corrected primary image matrix ($P1$) as a result of the primary image (table 9) and the result matrix (E^{D}) (table 14). Table 16 is the correction factor matrix K_0 calculated according to

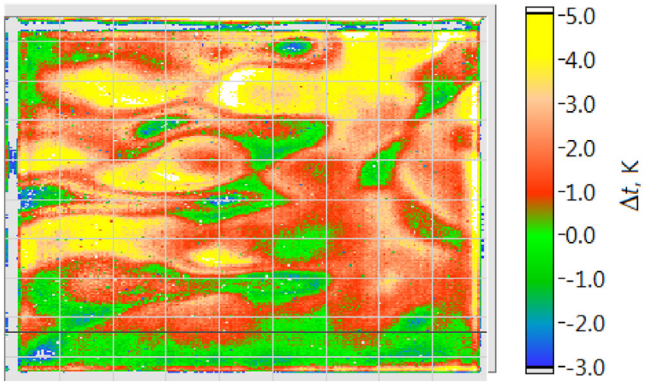

Figure 7. Nonuniformity of the responsivity of an imager working at 7.7 μm–9.3 μm, expressed in temperature at a radiance temperature of 320 °C, determined with the aid of the described method.

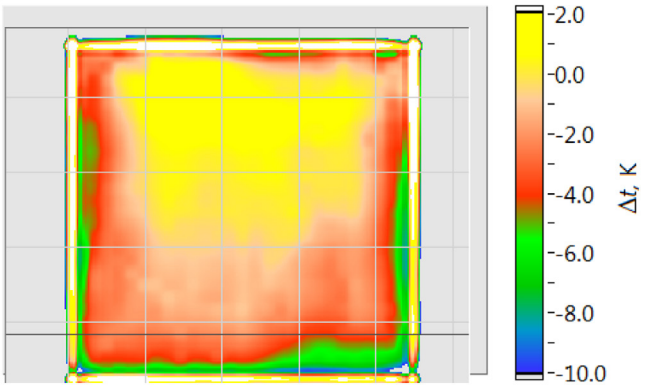

Figure 8. Nonuniformity of a plate radiator for a wavelength range of 7.7 μm–9.3 μm, at a radiance temperature of 320 °C, determined with the aid of the described method.

equation (19), normalized to the pixel response of the user-defined reference pixel in column 5 and row 5. The absolute response of the user-defined reference pixel in column 5 and row 5 of the imager is calibrated independently of the method of nonuniformity correction described here.

Table 17 is an 8 × 8 matrix describing the result matrix (E_{k1}^{D}) as a result of the 1st iteration. Table 18 is the corrected primary image matrix ($P2$) as a result of the primary image matrix ($P1$) (table 15) and the result matrix (E_{k1}^{D}) (table 17). Table 19 is the correction factor matrix K_1 calculated according to equation (34), normalized to the pixel response of the user-defined reference pixel in column 5 and row 5.

Table 20 is an 8 × 8 matrix describing the result matrix (E_{k2}^{D}) as a result of the 2nd iteration. Table 21 is the corrected primary image matrix ($P3$) as a result of the primary image matrix ($P2$) (table 18) and the result matrix (E_{k2}^{D}) (table 20). Table 22 is the correction factor matrix K_2 calculated according to equation (38), normalized to the pixel response of the user-defined reference pixel in column 5 and row 5. Table 23 is the relative deviation of the determined NUC to the predetermined values of the response characteristics.

4. Result of a practical determination

Figure 7 shows the result of a practical determination of the nonuniformity of the responsivity of the pixel of an imager with the described method calculated with the algorithm of the NUC difference method source, expressed in temperature. The used plate radiator was set to a temperature of 320 °C. Figure 8 shows the determined nonuniformity of the radiance temperature of the plate radiator with regard to figure 7. The plate radiator has an area of 300 mm × 300 mm.

5. Conclusion

We have presented a fast and direct method to perform the NUC of FPA-based imaging systems and, if required, also of scanning systems by applying a radiation source with an unknown and spatially nonhomogeneous radiance or radiance temperature distribution. The advantage of this method is that no information about the spatial radiance temperature distribution of the source is necessary. Only a sufficient temporal stability of the source to enable taking at least three successive pictures with the imaging system is required. The experimental procedure and the algorithm of the correction method leading to a relative response value of every pixel of the FPA in relation to a reference pixel has been described in detail. We illustrated the general method by a numerical example based on two 8 × 8 matrices representing an arbitrary nonhomogeneous source and an arbitrary nonhomogeneous FPA, respectively. An example of a practical realization of the described method with two images of the determined nonuniformities was represented. As this method can be easily and very generally applied to imaging systems, we think that it can lead to broad distribution to reduce fixed pattern noise (FPN) in all kinds of imager applications.

References

[1] Gutschwager B and Hollandt J 2015 Nonuniformity correction of imaging systems with a spatially nonhomogeneous radiation source *Appl. Opt.* **54** 10599–605
[2] Holst G C 2008 *Testing and Evaluation of Infrared Imaging Systems* 3rd edn (Maitland, FL: JCD Publishing Co)
[3] Ferrero A, Lopez M, Campos J and Sperling A 2014 Spatial characterization of cameras for low-uncertainty radiometric measurements *Metrologia* **51** 316–25
[4] Gutschwager B, Taubert D and Hollandt J 2015 Analysis of reference sources for the characterization and calibration of infrared cameras *Int. J. Thermophys.* **36** 303–14
[5] Gutschwager B, Cárdenas-García D and Hollandt J 2015 Determination of the responsivity non-uniformity of an infrared camera with regard to the measurement of radiance temperatures *Meas. Sci. Technol.* **26** 115402
[6] Verfahren zum Ermitteln von Korrekturparametern zum Korrigieren von Messwerten von Bildpunkten, um die Ungleichheit des Übertragungsverhaltens einzelner oder aller Bildpunkte eines Bildaufnahmesystems zu korrigieren *Deutsches Patent- und Markenamt* 10 2014 018 340.8, holder: PTB